Improvement of NOX removal efficiency using short-width pulsed power

doi: 10.1109/27.848102

Improvement of NO_X Removal Efficiency Using Short-Width Pulsed Power

Takao Namihira, Shunsuke Tsukamoto, Douyan Wang, Sunao Katsuki, Reuben Hackam, *Fellow, IEEE*, Hidenori Akiyama, *Fellow, IEEE*, Yoshitaka Uchida, and Masami Koike

***Abstract*—Pulsed power has been used to remove nitric oxide (NO) in a mixture of nitrogen, oxygen, and water vapor simulating the flue gases from a power station stack. The effect of the pulsewidth at a fixed applied voltage on NO removal concentration was studied. The dependence of the energy efficiency of the removal of NO at a fixed applied voltage on the pulsewidth, on the removal ratio of NO and on the discharge current was investigated. This removal energy efficiency increases with decreasing pulsewidth and decreasing removal ratio of NO.**

***Index Terms*—NO_X removal, NO removal energy efficiency, NO removal ratio, pulsed power.**

I. Introduction

THE APPLICATION of pulsed power to the central electrode of a coaxial cylindrical tube containing a gas at atmospheric pressure results in the production of nonthermal plasma. This produces high-energy electrons while the ambient temperature of the neutrals and ions remains relatively unchanged thus, reducing the energy consumption because most of the energy is utilized to create energetic electrons [1]–[11]. This was confirmed recently using spectroscopic measurements, which showed that for streamer pulses lasting less than 100 ns, the gas temperature in atmospheric nitrogen remained in the range 300–350K [12], [13]. The high-energy electrons produce chemical radicals that decompose the pollutant molecules of nitrogen oxides [1], [3], [5], [14]–[16]. Acid rain is partly produced by emissions of nitrogen oxides of NO and NO_2 originating from fossil burning fuels in thermal power stations, motor vehicles, and other industrial processes from steel production and chemical plants [15]–[20]. The efficient removal of NO_X and other gas pollutants has recently become of worldwide paramount importance. Nonthermal plasmas for removal of NO_X have been produced using an electron beam [2], [14], [20], a dielectric barrier discharge [18], [21], and a pulsed corona discharge [1]–[11], [22]–[25] at various energy effectiveness.

Manuscript received September 24, 1999; revised January 4, 2000. This work was supported by a Grant-in-aid for Scientific Research from the Ministry of Education of Japan.

T. Namihira and S. Katsuki are with the Department of Electrical and Computer Engineering, Kumamoto University, Kumamoto 860-8555, Japan.

H. Akiyama, S. Tsukamoto, and D. Wang are with the Graduate School of Science and Technology, Kumamoto University, Kumamoto 860-8555, Japan.

R. Hackam is with Kumamoto University, Kumamoto 860-8555, Japan. He is on leave from the Department of Electrical and Computer Engineering, University of Windsor, Windsor, ON N9B 3P4, Canada.

M. Koike and Y. Uchida are with the Research Laboratory, Kyushu Electric Power Co., Inc., Fukuoka 815-0032, Japan.

Publisher Item Identifier S 0093-3813(00)03666-3.

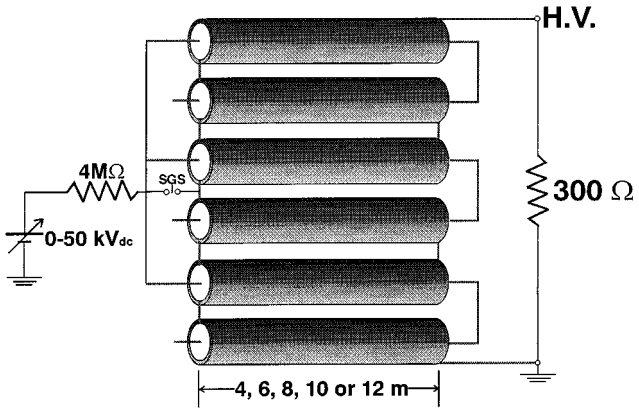

Fig. 1. Three-stage Blumlein generator showing the charging voltage (0–50 kV), the charging resistance (4 MΩ), the spark gap switch (SGS), and the matching output resistance (300 Ω). The cable length varied from 4–12 m giving pulsewidths of 40, 60, 80, 100, and 120 ns. Three hundred ohms was removed when coaxial reactor was used.

In the present work, a pulsed corona discharge has been used to obtain a high degree of NO removal efficiency. The effects of the pulsewidth, the pulse repetition frequency, and the discharge current on the percentage removal of NO and its energy efficiency are reported.

II. Experimental Setup and Procedure

A. Multistage Blumlein Generator

Fig. 1 shows a schematic diagram of a three-stage Blumlein generator used in the present work. Each stage consisted of two coaxial cables that had a characteristic impedance of 50 Ω (RG-213/U, Mitsubishi Densen, Japan). The length of the coaxial cable defines the pulsewidth. In this work, the setup had pulsewidths of about 40, 60, 80, 100, and 120 ns and corresponding lengths of coaxial cable of 4, 6, 8, 10, and 12 m. The width of the pulse is defined as the full-width at half-maximum (FWHM) of the voltage. The applied voltage from the Blumlein generator to the reactor was measured using a resistive voltage divider (1 Ω/5 kΩ, Ratio 5×10^3), which was connected between the central electrode and the ground (Fig. 2). The current to the reactor was measured using a Rogowski coil (Pearson current monitor, Model 2878, Pearson Electronics). A Hewlett Packard digital oscilloscope (HP 54542A) with a maximum band width of 500 MHz and a maximum sample rate of 2 G sample/s recorded the signals. The energy ($\int VI\,dt$) input to the discharge per pulse was determined from the digitized signals. V is the voltage across and I is the current through the reactor. The reactor was held at a height of 0.7 m from the

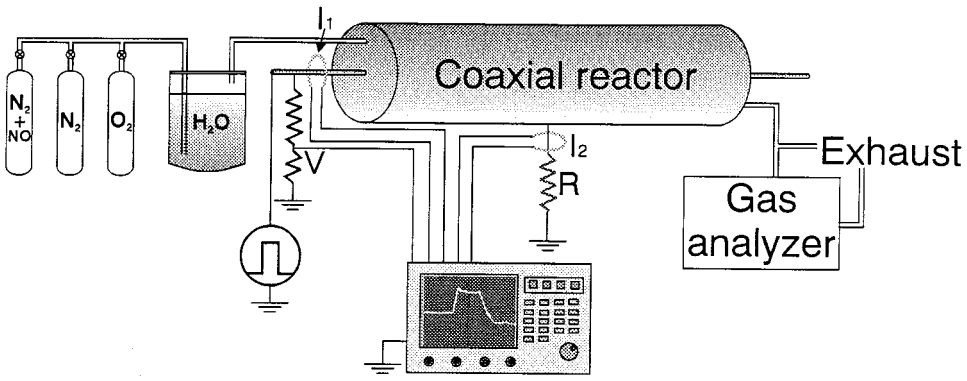

Fig. 2. Experimental set-up for removal of NO using a concentric electrodes reactor: I_1: current into the reactor; I_2, current in the external resistance R; value of R: 0, 50, 100, 200, and 300 Ω. Resistance divider, 1 Ω/5 kΩ.

ground. The current probe was located on the return current to the ground as shown in Fig. 2 when there was no resistance in series with the reactor $R = 0$. When a resistance was placed in series with the low voltage end of the reactor, the current probes were placed on the high-voltage end of the reactor and on the series resistance R as shown in Fig. 2. The oscilloscope was located inside a shielded room (70 dB) as this was necessary to reduce transient interference.

B. Treatment of Simulated Exhaust Gases

Fig. 2 shows the experimental setup. Gas cylinders of N_2, N_2 mixed with 0.09% NO, O_2, and H_2O were used to simulate exhaust gases from a thermal power station. The purity of the nitrogen cylinder was 99.99% and of the oxygen cylinder was 99.5% (Kumamoto Sanso, Japan). The amount of NO present in the flue gases depends on the type of fuel used and varies over a wide range. For a coal thermal power plant the amount of NO_X ($=NO + NO_2$) was reported to vary from 100 to 550 parts per million (ppm) parts of the gas mixture which was at 1.01×10^5 Pa and 70 °C–100 °C [4]. In a coal burning power plant, the NO concentration was also reported to be 250 ppm [22], [26] and that of NO_X 350 ppm [16], while the flue gases from heavy oil contained from 50 to 200 ppm of NO_X [20].

In the present work, the compositions of the simulated exhaust gases in the admixture were 200 ppm of NO, 5% O_2, 4% H_2O and the balance N_2 at 1×10^5 Pa and 25 ± 2 °C. The percentage of the pressure of water vapor (30.4 torr) in the gas mixture was determined by maintaining an ambient temperature of 29.2 °C of the water shown in Fig. 2 [27]. This was attained by allowing the gases to pass through water. The incorporation of water vapor in the gas mixture facilitated the conversion of NO to NO_2 [14] and NO_2 into nitric acid [14], [15]. The gas flow rate was fixed at 2.0 L/min (reduced to 273 K) at 1.01×10^5 Pa. A coaxial cylindrical reactor having a central rod made of stainless steel, 0.5 mm in diameter placed concentrically in a copper cylinder having 76 mm in internal diameter, and a length of 0.5 m was employed. A coaxial cylindrical reactor was used as it has been shown to be more effective in producing energetic electrons due to the generation of high-electrical fields near the wire [28], [29]. The energetic electrons are necessary to produce atomic nitrogen (N) and the radical OH by collisions with N_2 and H_2O, respectively [15]. In the present work, a positive voltage polarity was chosen for the central electrode of the reactor, since this was more effective than the negative polarity [1], [6]. A pulse repetition rate of 1–13 pps was used. The concentrations of NO and NO_2 were measured using a gas analyzer (Testo 33, Hodakatest, Japan) after a steady state was reached (within 5 min). The gas analyzer is based on the method of potentiostatic electrolysis. This method relies on the dependence of the current passing along the surface of a gold electrode immersed in sulfuric acid on the reactions of oxidation and deoxidation in the presence of various gases. The instrument was calibrated by the manufacturer.

III. Results and Discussion

A. Blumlein Generator

Fig. 3(a)–(e) shows typical waveforms of the voltage and current with varying pulsewidths in the nominal range from 40 ns [Fig. 3(a)] to 120 ns [Fig. 3(e)]. During this test a nominally matched load resistance of 300 Ω (50 $\Omega \times 2$ lines $\times$ 3 stages) was connected across the generator (Fig. 1). This resistance was removed when the coaxial discharge reactor was connected to the Blumlein generator. These pulsewidths were consistent (within $\pm 11\%$) with the calculated values from the lengths of the cable. The maximum value of the output voltage and the output current from the Blumlein generator for all pulsewidths, and without the coaxial reactor (Fig. 1), were at about the same level (Fig. 3). The maximum output voltage was 42.2 ± 1.1 kV and the maximum output current was 138.1 ± 5.5 A for all pulsewidths in the range 40–120 ns (Fig. 3). The negative voltage shown in Fig. 3 was due to the impedance mismatch between the Blumlein generator and its load formed by the 300 Ω (without the coaxial reactor), which originated from the stray capacitance and inductance as well as the connecting loads. When the parallel resistance was replaced by the coaxial reactor, the peak pulsed voltage was constant for all pulse widths from 40 to 120 ns at 49.2 ± 0.5 kV and the peak current varied in the range 88–175 A (Fig. 4).

B. Treatment of Simulated Gases

Fig. 4 shows typical waveforms of the applied voltage to and the discharge current in the coaxial reactor for varying pulsewidths. The peak of the voltage was almost the same

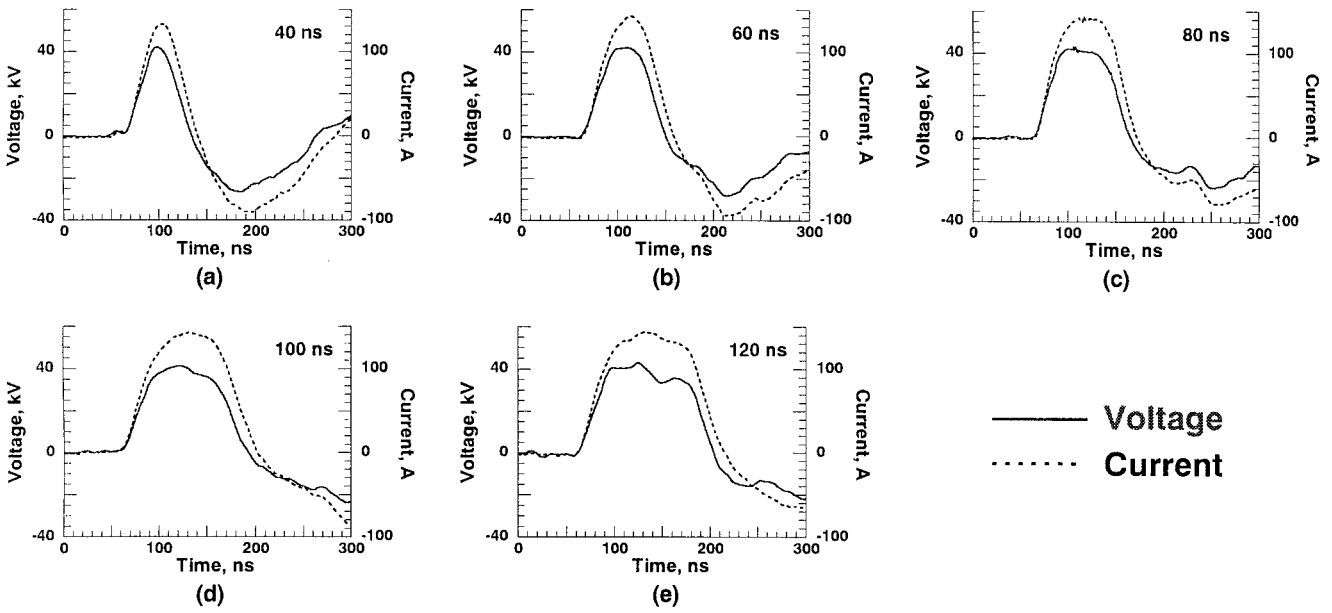

Fig. 3. Typical waveforms of voltage across and current through the load resistance of 300 Ω with varying pulsewidths in the range from 40 to 120 ns. Coaxial reactor was disconnected.

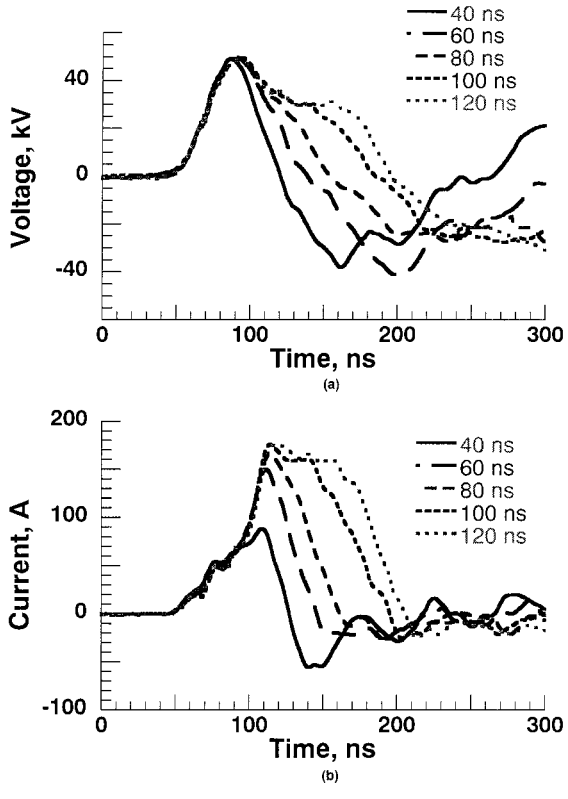

Fig. 4. (a) Applied voltage to and (b) discharge current in the coaxial reactor for varying pulsewidths. Conditions: gas pressure: 1.01×10^5 Pa; NO: 200 ppm; O_2: 5%; H_2O: 4%, and balance N_2 gas flow rate: 2.0 l/min; series resistance with reactor, 0 Ω. Parallel resistance was disconnected.

(49.2 kV ± 0.6 kV) for all pulsewidths in the range from 40 to 120 ns [Fig. 4(a)]. After the peak the behavior of the pulse for different widths varied due to the varying stored charge with varying capacitance of the Blumlein generator. Fig. 5 shows the input energy to the reactor for different pulsewidths and for duration of up to 300 ns when the current decreased to zero [Fig. 4(b)]. The input energy was calculated from the voltage and the current waveforms shown in Fig. 4. The input energy to the reactor was almost the same (Fig. 5) until the voltage reached its maximum value at about 90 ns (Fig. 4). Thereafter, the input energy was different for different pulsewidths (Fig. 5). Typically the energy delivered to the reactor after 300 ns of a single pulse having a width of 120 ns was about 0.49 J while that of the 40 ns pulsewidth was 0.18 J.

Fig. 6 shows the concentrations of NO and NO_2 as a function of time of application of the pulsed power. It will be observed that for 120 ns pulselength and 1 pps, it took about 3 min for the concentration of NO to decrease from 200 to 140 ppm, and then remained constant thereafter. The concentration of NO_2 increased steadily with time from 0 to 30 ppm (Fig. 6).

Fig. 7 shows the final concentrations of nitric oxide NO_f (a) and NO_2 (b) after applying pulsed powers of different widths and as a function of the repetition rate. NO_f is the final concentration of NO in the mixture after treatment with pulsed power. These measurements are reported here after a steady-state condition has reached in the concentrations of the gas constituents. This took less than 5 min (Fig. 6). It will be observed from Fig. 7(a) that the concentration of NO_f decreased with increasing pulse repetition rate and increasing pulsewidth from 40 to 120 ns. Typically, the concentration of NO_f decreased from its initial value from 200 to 156 ppm at 1 pps and to 9 ppm at 13 pps when the pulsewidth was 40 ns [Fig. 7(a)]. For a pulsewidth of 120 ns the concentration of NO_f decreased from an initial value of 200 to 4 ppm at 10 pps. This is a very effective removal of NO in the gas mixture and amounts to 98%. At a fixed repetition rate say of 7 pps, the concentration of NO_f decreased from 49 to 24 ppm with increasing pulselength from 40 to 120 ns, respectively [Fig. 7(a)]. The concentration of NO_2 increased steadily with increasing pulse rate up to 6 pps and slightly decreased thereafter [Fig. 7(b)].

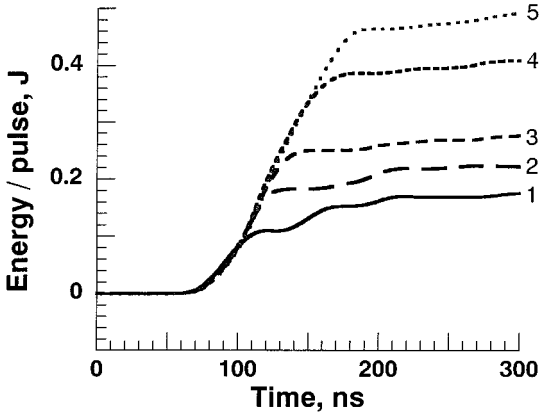

Fig. 5. Input energy to the coaxial reactor per pulse for different pulsewidths. Other conditions are as in Fig. 4.

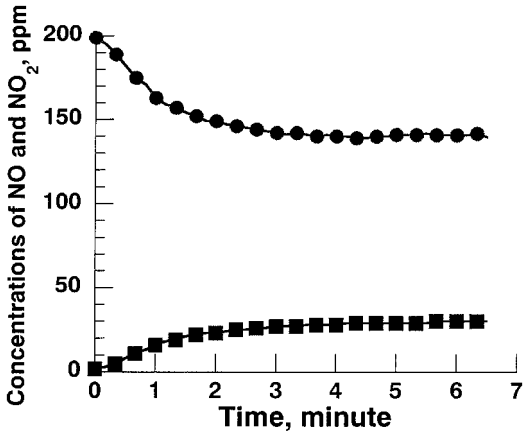

Fig. 6. Dependence of NO and NO_2 concentrations on time of application of pulsed power. Pulse rate: 1 pps; pulselength: 120 ns. Other conditions are as in Fig. 4. • NO, ■ NO_2.

C. Energy Efficiency of NO Removal

Fig. 8 shows the dependence of the energy efficiency of the removal of NO from the gas mixture in terms of mol/kWh. The percentage of the NO removal ratio NO_R (in %) is

$$NO_R = \frac{NO_i - NO_f}{NO_i} \times 100 \tag{1}$$

where NO_i (in ppm) and NO_f (in ppm) are the initial (before treatment) and the final (after treatment) concentrations of NO in the gas mixture, respectively. In the present work, $NO_i = 200$ ppm and the gas flow rate is fixed at 2.0 L/min (reduced to 273K). The energy efficiency of the removal of NO (NO_E, in mol/kWh) is given by

$$NO_E = \frac{\frac{2.0[\text{L/min}]}{22.4[\text{L/mol}]} \times (NO_i - NO_f) \times 60[\text{min/h}] \times 10^{-3}}{f \times E} \tag{2}$$

where f and E are the pulse repetition rate [pulses/s] and the input energy to the reactor per pulse [J/pulse], respectively. It should be noted that 0.03 kg of NO is equivalent to 1 mol and 0.0224 m^3 at 1.01×10^5 Pa and 273K. Fig. 8 shows the dependence of NO_E on NO_R for different pulsewidths in the range from 40 to 120 ns while maintaining the same peak pulsed voltage applied to the discharge reactor. It will be observed

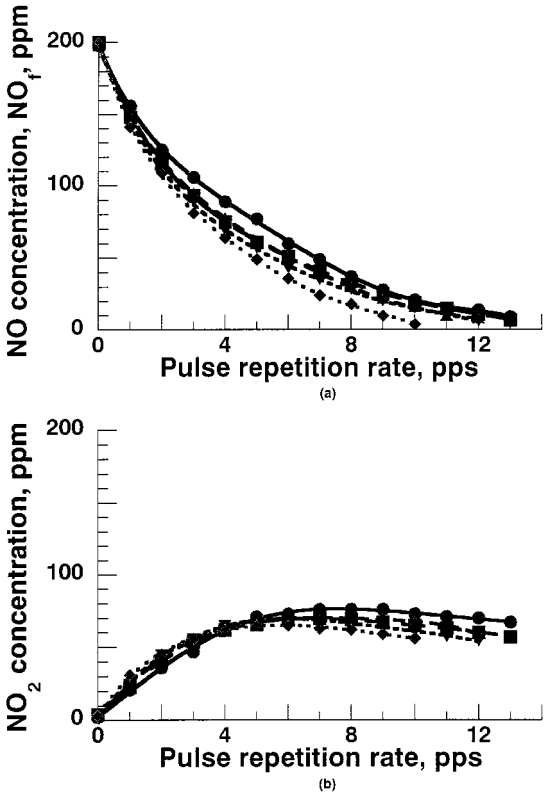

Fig. 7. Final concentrations of nitric oxide (a) NO_f and (b) NO_2 as a function of pulse repetition rate for different pulsewidths. Other conditions are as in Fig. 4. • 40 ns, ■ 60 ns, ♦ 80 ns, ▲ 100 ns, and ▼ 120 ns.

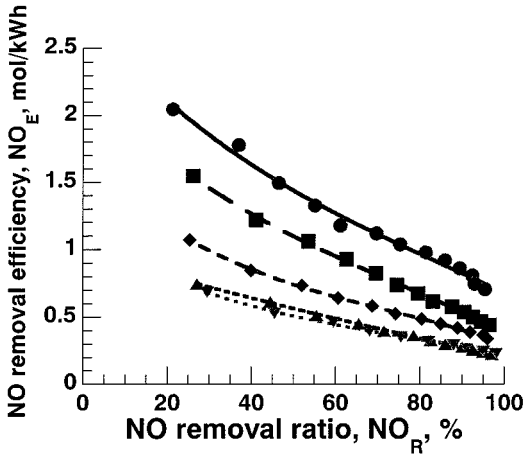

Fig. 8. Dependence of the energy efficiency of the removal of NO (mol/kWh) on the removal ratio of NO_R (1). Other conditions are as in Fig. 4. • 40 ns, ■ 60 ns, ♦ 80 ns, ▲ 100 ns, and ▼ 120 ns.

from Fig. 8 that the energy requirement (mol/kWh) of the NO removal increased and, therefore, the removal energy efficiency decreased with increasing NO removal ratio. The successive data in Fig. 8 (from left to right) with increasing NO_R were for pulse repetition rates from 1 to 13 pps. Fig. 8 shows that NO_E was higher for shorter pulsewidths at a fixed NO_R. This is because the input energy to the reactor decreased with decreasing pulsewidth (Fig. 5) while the change in $(NO_i - NO_f)$ (2) was relatively small as can be seen from Fig. 7(a), particularly for pulsewidths in the range from 40 to 100 ns. For the case of

40 ns, typically for $NO_R = 70\%$, ($f = 6$ pps), the value of $NO_E = 1.12$ mol/kWh (33.6 g/kWh) while for $NO_R = 23\%$, ($f = 1$ pps), NO_E increased to 2.08 mol/kWh [62.4 g/kWh] (Fig. 8).

The electrical energy requirement for the removal of NO is of a prime importance. The reduction of energy to an acceptable level will ensure a wide acceptance of the application of pulsed power for the removal of the NO pollutant. An attempt is made here to compare our results, wherever possible, to other results. For 90% removal of NO using 40 ns pulsewidth and 10 pps, Fig. 8 shows that 0.9 mol/kWh (27.0 g/kWh) was obtained. It was reported in [2] that for 90% removal of 100 ppm of NO in N_2 it was expended 83.7 J/L of N_2 using pulsed corona (100 ns) and 14 J/L using electron beam. These correspond to 5.76 g (of NO)/kWh and 34.4 g/kWh, respectively, using pulsed corona and electron beam methods. The yield (g/kWh) for the removal of NO using the pulsed corona method from the present study is comparable to that using the electron beam method [2].

In [4], using a coaxial reactor and pulsed power, the energy yield for 51% removal of NO_X was 20 g (of NO)/kWh when the initial value of NO had been 515 ppm in a mixture of N_2, CO, O_2, ammonia, and H_2O. In [23], the energy yield of NO removal (initial value, 180 ppm) using negative pulsed corona at 50 pps without moisture in the air was also 20 g/kWh which was substantially higher than that of 3–5 g/kWh using dc corona. It was reported that to remove about 90% of an initial value of 213 ppm of NO in a mixture with ethylene using pulsed corona of 200 ns width in a coaxial reactor the yield was 33.3 g/kWh [6, Fig. 8]. The latter value is very close to that of 34.4 g/kWh reported in [2] for 90% removal of NO with initial value of 100 ppm using an electron beam. In a mixture of 5% O_2, 10% H_2O, 15% CO_2, 70% N_2, and initial concentration of 720 ppm of NO and a molar ratio of n-octane to NO of 4 : 1, a yield of 59.5 g (NO)/kWh [16 Wh/m^3 (of gas mixture)] was obtained at a gas temperature of 114 °C using pulsed power [30].

The present study clearly indicates that the yield of the pulsed corona is comparable with the yield value reported using electron beam irradiation [2] for the case when other additives such as ammonia, n-octane, ethylene, or CO_2 are not employed. A cost comparison, sponsored by Japan Ministry of International Trade and Industry, for the removal of 300 ppm of NO from a thermal power plant employing coal at a power capacity of 250 MW and using pulsed corona, electron beam, and calcium/gypsum process with ammonia concluded that the pulsed corona is the most feasible and most economical of the three methods [31]. Some details on the cost analysis and the results obtained maybe gleaned from [31].

D. Development of the Pulsed Discharge

An optical quartz fiber (400 μm in core diameter) was set at a position very close to the central electrode and connected to a photomultiplier tube (PMT) (type R166UH, Hamamatsu, Japan) to observe the light emission from the discharge as a function of time and correlate it with the measurements of the applied voltage and discharge current. Various times are identified on the waveforms of Fig. 9 in the development of the discharge in the coaxial reactor. In Fig. 9, a is the onset of the applied voltage to the electrodes, b is the time in which the light

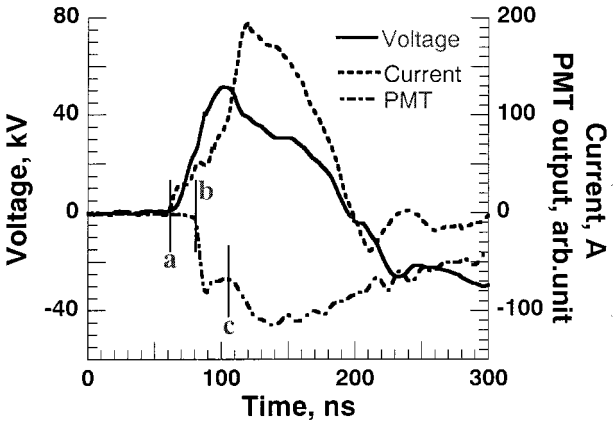

Fig. 9. Applied voltage, discharge current, and photo multiplier tube (PMT) current as a function of time during the application of a single power pulse to the coaxial reactor. Times a to c are defined in the text. Nominal pulsewidth, 100 ns; other conditions are as in Fig. 4.

emission started to develop, and c corresponds to the peaks of the PMT output and the Blumlein voltage pulse and approximately the arrival time of a streamer to the outer electrode. The time of arrival of the streamer at the outer electrode is inferred from a subsidiary experiment in another reactor having a length of 1 cm, a wire of 0.5 mm in diameter, and an outer diameter of 76 mm where the optical fiber was located in successively increasing radii from the positive central electrode. The dimensions of these electrodes were the same as in the present reactor except for the length of the reactor. In the present paper, the fiber is located near the wire and thus a distant away from the cylinder. The observed minimum in the light emission near the wire at time c (Fig. 9) thus coincides approximately with the arrival of the streamer at the outer electrode. After time c the conductivity of the plasma (dI/dt, where I is the current in and V the voltage across the gap) increased substantially due to the simultaneous increase of the discharge current and the decrease of the applied voltage. The dependence of the current I on time t was determined by the impedances of the reactor tube and the discharge in the gas. The impedance was largely capacitive before the onset of the discharge. During the discharge the impedance became complex and the current was determinedly by

$$V = RI + L\frac{dI}{dt} + \frac{1}{c}\int I\,dt \tag{3}$$

where

R the resistance;
L the inductance;
C the capacitance of the reactor during the discharge.

Fig. 9 shows that at the vicinity of time c the current I and dI/dt increased rapidly while the change in V was relatively small. Therefore, since the second and third terms of (3) increased and also I increased in the first term, R must decrease to satisfy a smaller change in V and thus the conductivity increased with increasing current.

The average velocity of the streamer may be calculated from the gap distance between the electrode (37.75 mm) and the time c–$b = 21$ ns (Fig. 9) to be about 1.8×10^6 m/s. The value of the time that it took for the streamer to arrive to the outer electrode

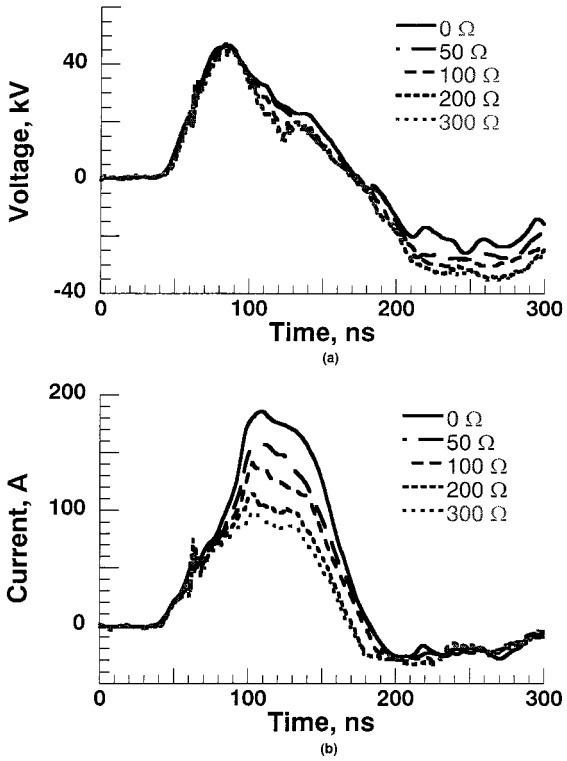

Fig. 10. Dependence of (a) applied voltage and (b) discharge current on series resistance with the coaxial reactor. Nominal pulsewidth, 100 ns; other conditions are as in Fig. 4. Peak currents: 0 Ω (185 A); 50 Ω (156 A); 100 Ω (137 A); 200 Ω (114 A); 300 Ω (98 A).

is, in general, consistent with the values of the time lag to breakdown from the streamer theory as summarized by Kunhardt and Luessen [32]. Recently, both a measured and a calculated value of about 1×10^6 m/s was reported for the streamer velocity at a location close to the wire of a coaxial tube in a mixture of 10% oxygen with N_2, at a pulsed voltage of 25 kV [12]. In the latter study, the streamer velocity was found to increase with decreasing oxygen concentration from 40% to 10%. Since in the present work 5% oxygen and 40 kV pulsed voltage were used, our higher value for the streamer velocity may be considered to be consistent with that reported in [12].

E. Effect of Discharge Current on Removal of NO_X

A resistance in the range from 0 to 300 Ω was connected in series with the coaxial reactor to the ground in order to investigate the effect of the discharge current level on the removal of NO. In this part of the study the currents were measured on the high voltage side at the input to the central wire electrode and in the external resistance (Fig. 2). This was done to mitigate against possible errors that might be present due to parallel capacitance paths between the outer cylinder and the ground when a resistance is connected there. The voltage was measured across both the reactor and the external resistance using the resistance divider (Fig. 2). The voltage across the reactor was calculated by subtracting the voltage drop across the external resistance from the measured voltage between the central electrode and the ground. The energy fed into the corona discharge was calculated using the voltage across and the current flowing into the reactor. Fig. 10(a) shows that the series resistance has only a small influence on the shape and the peak of the voltage pulse. Fig. 10(b) shows that the series resistance has, and as expected, a strong influence on the value of the peak current. The peak current typically varied from 185 A with 0 Ω to 98 A with 300 Ω. Fig. 11 shows the discharge current I_1 in the coaxial reactor and the current I_2 in the external series resistance. It will be observed from a comparison of the currents shown in Fig. 11 that the presence of capacitive paths for the currents in parallel with the external resistance is not significant. Fig. 12 shows the input energy to reactor calculated from voltage and current in Fig. 10 for different series resistances. The input energy to the reactor decreased with increasing series resistance. Typically, the input energy with 300 Ω in series with the coaxial reactor was about 60% of that when there was no resistance in series (0.46 J/pulse) while maintaining all other conditions the same (Fig. 11).

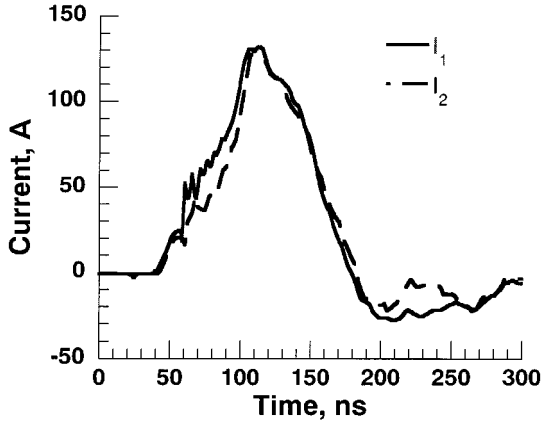

Fig. 11. Dependence of the discharge current I_1 in the coaxial reactor and I_2 in the resistance R placed in series with the reactor (Fig. 2) on time. Conditions: R, 50 Ω.

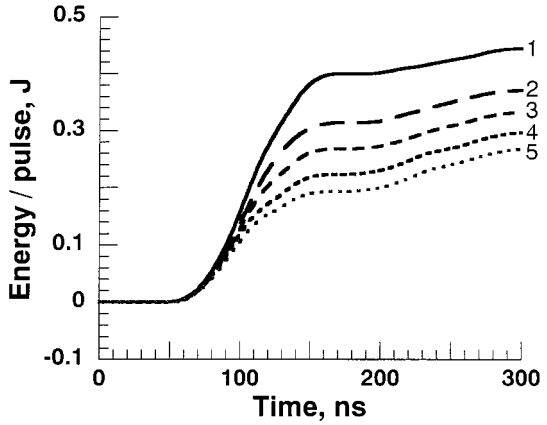

Fig. 12. Input energy to the coaxial reactor per pulse for different series resistances with the coaxial reactor. Nominal pulsewidth, 100 ns; other conditons are as in Fig. 4. curve 1, 0 Ω (185 A); curve 2, 50 Ω (156 A); curve 3, 100 Ω (137 A); curve 4, 200 Ω (114 A); and curve 5, 300 Ω (98 A).

Fig. 13 shows the final concentrations of NO_f (a) and NO_2 (b) as a function of the pulse repetition rate for different values of the series resistance. The initial value of NO in the mixture was 200 ppm. It will be observed that more NO was removed with decreasing series resistance for a fixed pulse rate. Typically, for 10 pps the final value of NO was 36 ppm for 300 Ω (peak current 98 A) and 17 ppm when there was no series resistance (185 A).

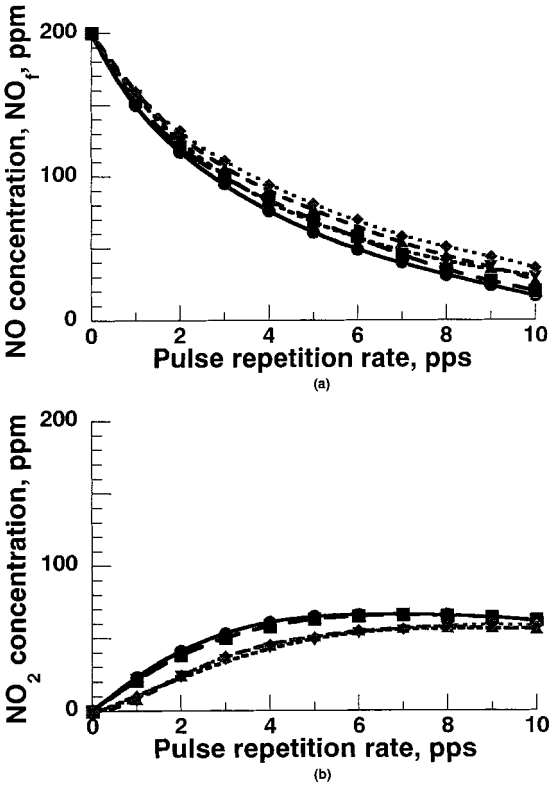

Fig. 13. Final concentrations of nitric oxide, (a) NO_f and (b) NO_2 as a function of the pulse repetition rate for different series resistances (and peak currents) with the coaxial reactor. Nominal pulsewidth, 100 ns; other conditions are as in Fig. 4. • 0 Ω (185 A), ■ 50 Ω (156 A); ♦ 100 Ω (137 A), ▲ 200 Ω (114 A), and ▼ 300 Ω (98 A).

This was due to the increased current [Fig. 10(b)] and increased energy (Fig. 12) with decreasing series resistance. The concentration of NO decreased with increasing pulse repetition rate for all series resistance values.

Fig. 14 shows the energy efficiency of the removal of NO as a function of the removal ratio of NO for different resistance values placed in series with the reactor. It will be observed from Fig. 14 that a higher removal efficiency was obtained at a given removal ratio of NO, with increasing resistance from 0–300 Ω and therefore with decreasing discharge current. This is because the energy fed into the discharge decreases with increasing resistance (Fig. 12) while the effect of the latter on the removal of NO is relatively small [Fig. 13(a)] and thus the energy yield (mol/kWh) increases with decreasing current (Fig. 14). It should be mentioned that in calculating the energy efficiency (Fig. 14) only the energy input to the gas mixture was taken into account and that dissipated in the resistance was not considered. The effect on the removal of NO with changing either the pulsewidth [Fig. 7(a)] or the peak current [Fig. 13(a)] is relatively small. This is because the initial development of the pulse current is practically the same for all pulsewidths [Fig. 7(a)] and pulse currents [Fig. 13(a)]. The streamer propagation in the gap is largely determined by the initial development of the pulse current [Figs. 4(b) and 10(b)]. The present results that show an increase in the energy requirement with increasing the removal ratio of NO (Figs. 8 and 14) are consistent with the recently reported measurements in a mixture of air, water, and NO using pulsed corona in a wire-plate electrode structure [33].

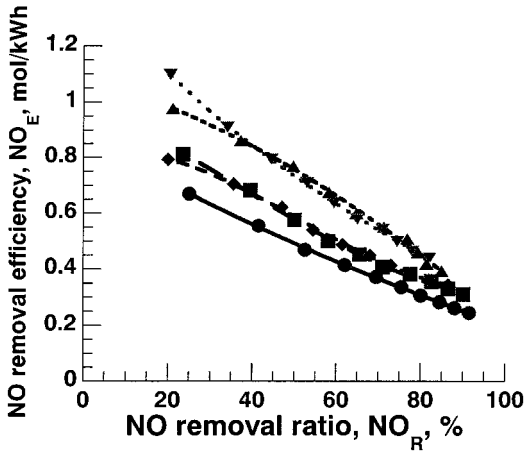

Fig. 14. Dependence of the energy efficiency of the removal of NO (NO_E) on the removal ratio or NO for different discharge currents. Pulsewidth, 100 ns; other conditions are as in Fig. 4. • 0 Ω (185 A), ■ 50 Ω (156 A), ♦ 100 Ω (137 A), ▲ 200 Ω (114 A), and ▼ 300 Ω (98 A).

IV. Conclusion

Pulsed power at short durations (40–120 ns) has been used to remove NO in a mixture of N_2, O_2, and H_2O. The following conclusions have been deduced:

1) the energy required to remove NO decreased with decreasing pulsewidth;
2) the effect on the removal of NO with changing either the pulsewidth or the peak current is relatively small;
3) the energy removal efficiency of NO using 40-ns duration of pulsed power is comparable to that of the electron beam method.

References

[1] S. Masuda, "Pulse corona induced plasma chemical process: A horizon of new plasma chemical technologies," *Pure Appl. Chem.*, vol. 60, pp. 727–731, 1988.

[2] B. M. Penetrante, M. C. Hsiao, J. N. Bardsley, B. T. Merritt, G. E. Vogtlin, P. H. Wallman, A. Kuthi, C. P. Burkhart, and R. J. Bayless, "Electron beam and pulsed corona processing of volatile organic compounds and nitrogen oxides," in *Proc. 10th IEEE Int. Pulsed Power Conf.*, Albuquerque, NM, 1995, pp. 144–149.

[3] H. Akiyama, K. Kawamura, T. Takeshita, S. Katsuki, S. Maeda, S. Tsukamoto, and M. Murata, "Removal of NO_X using discharges by pulsed power," in *Proc. 10th IEEE Int. Pulsed Power Conf.*, Albuquerque, NM, 1995, pp. 133–137.

[4] G. Dinelli, L. Civitano, and M. Rea, "Industrial experiments on pulse corona simultaneous removal of NO_X and SO_2 from flue gas," *IEEE Trans. Indust. Appl.*, vol. 26, pp. 535–541, 1990.

[5] J.-S. Chang, P. A. Lawless, and T. Yamamoto, "Corona discharge processes," *IEEE Trans. Plasma Sci.*, vol. 19, pp. 1152–1166, 1991.

[6] E. J. M. van Heesch, H. W. M. Smulders, S. V. B. van Paasen, P. P. M. Blom, F. M. van Gompel, A. J. P. M. Staring, and K. J. Ptasinski, "Pulsed corona for gas and water treatment," in *Proc. 11th IEEE Int. Pulsed Power Conf.*, Baltimore, MD, 1997, pp. 103–108.

[7] J. S. Clements, A. Mizuno, W. C. Finney, and R. H. Davis, "Combined removal of SO_2, NO_X and fly ash from simulated flue gas using pulsed streamer corona," *IEEE Trans. Indust. Appl.*, vol. 25, pp. 62–69, 1989.

[8] S. Masuda and H. Nakao, "Control of NO_X by positive and negative pulsed corona discharges," *IEEE Trans. Indust. Appl.*, vol. 26, pp. 374–383, 1990.

[9] A. Mizuno, K. Shimizu, A. Chakrabarti, L. Dascalescu, and S. Furuta, "NO_X removal process using pulsed discharge plasma," *IEEE Trans. Indust. Appl.*, vol. 31, pp. 957–963, 1995.

[10] H. Akiyama, "Pollution control by pulsed power," in *Proc. 1995 Int. Power Electron. Conf.*, Yokohama, Kanagawa, Japan, 1995, pp. 1397–1400.

[11] H. Akiyama, Y. Nishihashi, S. Tsukamoto, T. Sueda, S. Katsuki, M. Hagler, J. C. Dickens, and N. Inoue, "Streamer discharges by pulsed power on a spiral transmission line," in *Proc. 11th IEEE Int. Pulsed Power Conf.*, Baltimore, MD, 1997, pp. 109–114.
[12] Y. L. M. Creyghton, E. M. van Veldhuizen, and W. R. Rutgers, "Electrical and optical study of pulsed positive corona," in *Non-Thermal Plasma Techniques For Pollution Control*, B. M. Penetrante and S. E. Schultheis, Eds. New York: Springer-Verlag, 1993, pt. A, pp. 205–230.
[13] K. Kawamura, S. Tsukamoto, T. Takashita, S. Katsuki, and H. Akiyama, "NO_X removal using inductive pulsed power generator" (in Japanease), *Trans. IEEJ*, vol. 117-A, pp. 956–961, 1997.
[14] B. M. Penetrante, "Removal of NO_X from diesel generator exhaust by pulsed electron beams," in *Proc. 11th IEEE Int. Pulsed Power Conf.*, Baltimore, MD, USA, 1997, pp. 91–96.
[15] K. Urashima, J.-S. Chang, J.-Y. Park, D.-C. Lee, A. Chakrabarti, and T. Ito, "Reduction of NO_X from natural gas combustion flue gases by corona discharge radical injection techniques," *IEEE Trans. Indust. Appl.*, vol. 34, pp. 934–939, 1998.
[16] B. M. Penetrante, "Pollution control applications of pulsed power technology," in *9th IEEE Int. Pulsed Power Conf.*, Albuquerque, NM, 1993, pp. 1–5.
[17] I. Gallimberti, "Impulse corona simulation for flue gas treatment," *Pure Appl. Chem.*, vol. 60, pp. 663–674, 1988.
[18] K. Urashima, J.-S. Chang, and T. Ito, "Reduction of NO_X from combustion flue gases by superimposed barrier discharge plasma reactors," *IEEE Trans. Indust. Appl.*, vol. 33, pp. 879–886, 1997.
[19] D. Bhasavanich, S. Ashby, C. Deeney, and L. Schlitt, "Flue gas irradiation using pulsed corona and pulsed electron beam technology," in *Proc. 9th IEEE Int. Pulsed Power Conf.*, Albuquerque, NM, 1993, pp. 441–444.
[20] J.-S. Chang, P. C. Looy, K. Nagai, T. Yoshioka, S. Aoki, and A. Maezawa, "Preliminary pilot plant tests of a corona discharge-electron beam hybrid combustion flue gas cleaning system," *IEEE Trans. Indust. Appl.*, vol. 32, pp. 131–137, 1996.
[21] L. Rosocha, G. K. Anderson, L. A. Bechtold, J. J. Coogan, H. G. Heck, M. Kang, W. H. McCulla, R. A. Tennant, and P. J. Wantuck, "Treatment of hazardous organic wastes using silent discharge plasmas," in *Non-Thermal Plasma Techniques for Pollution Control*, B. M. Penetrante and S. E. Schultheis, Eds. New York: Springer-Verlag, 1993, pt. B, pp. 281–308.
[22] S. Tsukamoto, T. Namihira, D. Wang, S. Katsuki, H. Akiyama, E. Nakashima, A. Sato, Y. Uchida, and M. Koike, "NO_X and SO_2 removal by pulsed power at a thermal power plant," in *Proc. 12th IEEE Int. Pulsed Power Conf.*, Monterey, CA, June 1999, to be published.
[23] S. Masuda and H. Nakao, "Control of NO_X by positive and negative pulse corona discharges," *IEEE Trans. Indust. Appl.*, vol. 26, pp. 374–383, Feb. 1990.
[24] S. Tsukamoto, T. Namihira, D. Wang, S. Katsuki, H. Akiyama, E. Nakashima, A. Sato, Y. Uchida, and M. Koike, "Pollution control of actual flue gas using pulsed power at a thermal power plant" (in Japanese), *Trans. IEEJ*, vol. 119-A, pp. 984–989, 1999.
[25] T. Namihira, D. Wang, S. Tsukamoto, S. Katsuki, and H. Akiyama, "Effect of gas composition for NO_X removal using pulsed power" (in Japanese), Trans. IEEJ, vol. 119-A, 1999, to be published.
[26] L. Civitano, "Industrial application of pulsed corona processing to flue gas," in *Non-Thermal Plasma Techniques For Pollution Control*, B. M. Penetrante and S. E. Schultheis, Eds. New York: Springer-Verlag, 1993, pt. B, pp. 103–130.
[27] R. C. Weast, Ed., *CRC Handbook of Chemistry and Physics*, 65th ed., 1984–1985, p. D-193.
[28] R. Hackam, "Total secondary ionization coefficient and breakdown potentials of hydrogen, methane, ethylene, carbon monoxide, nitrogen, oxygen and carbon dioxide between mild steel coaxial cylinders," *J. Phys. B: Atom. Mol. Phys.*, vol. 2, pp. 216–233, 1969.
[29] R. Hackam, "Total secondary ionization coefficients and breakdown potentials of monatomic gases between mild steel coaxial cylinders," *J. Phys. B: Atom. Mol. Phys.*, vol. 2, pp. 201–215, 1969.
[30] G. E. Vogtlin and B. M. Penetreante, "Pulsed corona discharge for removal of NO_X from flue gas," in *Non-Thermal Plasma Techniques for Pollution Control*, B. M. Penetrante and S. E. Schultheis, Eds. New York: Springer-Verlag, 1993, pt. B, pp. 187–198.
[31] S. Masuda, "Report on novel dry $DeNO_X$/$DeSO_X$ technology for cleaning combustion gases from utility thermal power plant boilers," in *Non-Thermal Plasma Techniques for Pollution Control*, B. M. Penetrante and S. E. Schultheis, Eds: Springer-Verlag, 1993, pt. B, pp. 131–137.
[32] E. E. Kunhardt and L. H. Luessen, "Electrical breakdown and discharges in gases," in *Fundamental Processes And Breakdown*. New York: Plenum, 1981, pp. 255–256.
[33] Y. S. Mok, S. W. Ham, and I. S. Nam, "Evaluation of energy utilization efficiencies for SO_2 and NO removal by pulsed corona discharge process," *Plasma Chem. Plasma Processing*, vol. 18, pp. 535–550, 1998.

Takao Namihira was born in Shizuoka, Japan, on January 23, 1975. He received the B.S. and M.S. degrees from Kumamoto University, Kumamato, Japan, in 1997 and 1999, respectively.

Since 1999, he has been a Research Associate at Kumamato University.

Shunsuke Tsukamoto was born in Kumamato, Japan, on July 3, 1954. He graduated from the Department of Electrical Engineering of the Ariake National College of Technology, Fukuoka, Japan, in 1975. He received the M.S. degree from Kumamato University, Japan, in 1998, where he is currently working toward the Ph.D. degree.

He is also currently an Assistant Professor of Ariake National College of Technology.

Douyan Wang was born in Beijing, China, on May 18, 1975. She received the B.S. degree in electrical engineering in 1998 from Kumamato University, Kumamoto, Japan, where she is currently pursuing the M.S. degree.

Sunao Katsuki was born in Kumamato, Japan, on January 5, 1966. He received the B.S., M.S., and Ph.D. degrees from Kumamato University, Kumamato, Japan, in 1989, 1991, and 1998, respectively.

From 1991–1998, he was a Research Associate at Kumamato University. Since 1998, he has been an Associate Professor at Kumamato University.

Reuben Hackam (M'76–SM'76–F'88) received the B.S. degree from the Technion, Israel Institute of Technology, Israel in 1960 and the Ph.D. and D.Eng. degrees from the University of Liverpool, England in 1964 and 1988, respectively.

From 1964 to 1968, he was with General Electric–English Electric Company, Stafford, England. From 1969 to 1978, he was with the University of Sheffield and since 1979 he has been a Professor of electrical engineering at the University of Windsor, Canada, where he holds the position of University Distinguished Professor. During 1998–1999 he was on sabbatical leave at the Kumamato University, Japan.

Hidenor Akiyama (M'87–SM'99–F'99) was born in Ehime, Japan, on April 2, 1951. He received the B.S. degree in electrical engineering from the Kyushu Institute of Technology, Fukuoka, Japan, in 1974, and the M.S. and Ph.D. degrees from Nagoya University, Japan, in 1976 and 1979, respectively.

From 1979 to 1985, he was a Research Associate at Nagoya University. In 1985, he joined the faculty at Kumamato University, Kumamato, Japan, where he is currently a Professor.

Yoshitaka Uchida was born in Fukuoka, Japan, on September 24, 1960. He received the M.E. degree in material science from Kyushu University, Japan, in 1985. The same year, he joined Kyushu Electric Power Co., Inc., Fukuoka, Japan, and is now the Senior Research Engineer of the Power Plant Engineering Group in the Research Laboratory.

Masami Koike was born in Fukuoka, Japan, on February 17, 1952. He received the M.E. degree in applied chemistry from Kyushu University, Japan, in 1976. The same year, he joined Kyushu Electric Power Co., Inc., Fukuoka, Japan, and is now the Principal Research Engineer of the Power Plant Engineering Group in the Research Laboratory.